

## Superposition of decaying flux distributions: A memory effect from flux creep

M. N. Kunchur and S. J. Poon

*Department of Physics, University of Virginia, Charlottesville, Virginia 22901*

M. A. Subramanian

*Central Research and Development, E. I. duPont de Nemours and Company, Experimental Station, Wilmington, Delaware 19898*

(Received 19 October 1989)

A model is presented that considers the magnetic relaxation from thermally activated flux creep in a superconductor, after the application of two consecutive field steps separated by a waiting time  $t_w$ . The time evolution of the resulting superposition of flux distributions is expected to show a characteristic inflection point at a time  $t'_i$ . The behavior is reminiscent of, but fundamentally different from, the memory effect of the superconducting-glass model. Measurements on  $\text{Bi}_2\text{Sr}_2\text{CaCu}_2\text{O}_{8+\delta}$  single crystals show the predicted temperature and field dependence of  $t'_i$ .

Recently there has been considerable interest in the magnetic properties of high- $T_c$  superconductors. Early work by Müller, Takashige, and Bednorz<sup>1</sup> on magnetic irreversibility and relaxation showed that the behavior was consistent with that of a superconducting glass: a model proposed by Ebner and Stroud<sup>2</sup> that describes the behavior of weakly linked superconducting clusters.

Subsequently Yeshurun and Malozemoff<sup>3</sup> showed that a conventional critical-state-flux-creep type of model could also explain these properties. In the critical-state model<sup>4,5</sup> the initial profile of the flux density  $B$  depends only on the applied field  $H$ , and its history—with the local critical-current-density (magnitude) given by  $J_c(B) = (c/4\pi)|dB/dx|$  (Maxwell's equations). Measurements of remanent magnetization<sup>6,7</sup> support that description. As a result of flux creep, the slope of the profile decreases leading to a time-dependent magnetization  $M(t)$ .<sup>8,9</sup> The flux-pinning well depth  $U_0$ , determined from  $M(t)$ , has served as an important parameter in the comparison of different materials.<sup>7,10</sup>

Recent theoretical<sup>11</sup> and experimental work<sup>12</sup> has shown that the properties of the flux lattice and the character of the flux pinning in high- $T_c$  superconductors might be quite unconventional. Additionally, Rossel, Maeno, and Morgenstern<sup>13</sup> have observed memory effects in Y-Ba-Cu-O single crystals supporting a superconducting-glass picture—at least in their temperature and field ranges.

The preceding discussion indicates the ambiguity in the correct description for the magnetic relaxation in high- $T_c$  superconductors, and raises the question whether the conventional flux-creep model is applicable even at low temperatures. In this work we show that a memory effect similar to that predicted by the superconducting-glass model is also to be expected from the flux-creep model. When a zero-field-cooled (ZFC) superconductor is subjected to two consecutive field changes (0 to  $H_1$  and  $H_1$  to  $H_2$ ) separated by a waiting time  $t_w$ , the subsequent decay of magnetization shows an inflection or crossover point at a time  $t'_i$ . In the superconducting-glass model  $t'_i \approx t_w$ . In the memory effect derived here,  $t'_i$  in general does not equal  $t_w$ , but is a function of the four param-

eters,  $t_w$ ,  $T$ ,  $H_1$ , and  $H_2$ . We present data that are consistent with the model's predictions.

The single crystals of  $\text{Bi}_2\text{Sr}_2\text{CaCu}_2\text{O}_{8+\delta}$  (preparation described in Refs. 14 and 15) were platelets ( $c$  axis along the small dimension) with approximate dimensions  $1 \times 1 \times 0.1$  mm<sup>3</sup>. Previous magnetic measurements on crystals from this batch were reported earlier.<sup>7,15</sup> Two crystals were mounted on a sheet of mylar with the CuO planes aligned parallel to the field. The contribution of the sample holder was negligible ( $< 0.05\%$  of total signal). Magnetic moments were measured in a superconducting-quantum-interference-device susceptometer (SHE model 905).

We will now proceed to calculate the relation between  $T$ ,  $H_1$ ,  $H_2$ ,  $t_w$ , and  $t'_i$ .  $J_c$  will be assumed to be independent of field (i.e., the flux-density profiles are linear as in the Bean model<sup>4</sup>) since other models and empirical critical-state relations yield the Bean approximation in their low-field limits.<sup>5,16</sup> Modifications to the results arising from other profile shapes will be discussed. When the CuO planes are parallel to the field, it was shown in our previous work<sup>7</sup> that flux penetration and creep occur predominantly parallel to the planes (i.e., flux enters the platelet through the ends): The problem then reduces to that of an infinite slab whose "thickness" equals the width  $w$ , of the crystal. The case when the field is parallel to the  $c$  axis is complicated by the large field-dependent demagnetizing factor and will not be treated here.  $H_{c1}$  ( $\sim 10$  Oe) (Refs. 7 and 15) will be neglected ( $H_1, H_2 \sim 300$  Oe).

Figure 1(a) shows the initial flux-density profiles in a sample (only half shown for symmetry reasons) for different fields. Because  $|dB/dx| = 4\pi J_c/c$ , the field penetrates to a depth  $X = cH/(4\pi J_c)$ , from the surface of the sample.  $H^* = 2\pi w J_c/c$  is the field for complete flux penetration (for  $T \approx 10$  K,  $H^* \approx 1$  kOe). The analysis that follows applies to the case of incomplete flux penetration at all times.

Figure 1(b) shows how the flux-density profile, created by applying the first field  $H_1$ , evolves with time. Thermally activated flux creep causes the slope to decrease with time, as expressed by the following time- and

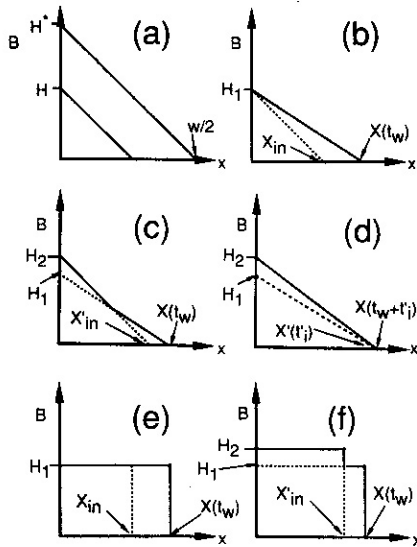


FIG. 1. Flux-density ( $B$ ) profiles in a sample of width  $w$  (half shown)  $t$  and  $t'$  are times measured after the applications of fields  $H_1$  and  $H_2$ , respectively. (a) Initial profiles for different applied fields. Complete flux penetration occurs at  $H^*$ . (b) Initial and time-evolved profiles after applying  $H_1$ . (c) Superposition of initial profile of  $H_2$  over time-evolved profile of  $H_1$ . (d) Aged compound profile of (c) at the time  $t'_i$ . (e) and (f) Similar behavior for hypothetical rectangular profiles.

temperature-dependent form of  $J_c$ :<sup>3,9</sup>

$$J_c = J_{c0} \left[ 1 - \left( \frac{k_B T}{U_0} \right) \ln \left( \frac{t}{t_0} \right) \right] \quad (1)$$

Here  $t_0$  is a parameter involving the fluxon-oscillation frequency, mean fluxon hopping distance, etc. Equation (1) is valid<sup>17</sup> in the limit of large driving forces when  $U_0 \gg kT$  (here  $U_0/kT \sim 50$ ). Normally  $J_c$  is evaluated at some arbitrary initial time  $\delta$  (5–15 min), after a field change. This initial nominal value of  $J_c$  will be called  $J_{c,in}$  ( $H^*$  then is  $2\pi w J_{c,in}/c$ ). By inserting Eq. (1) into  $X = cH/(4\pi J_c)$ , and keeping the two leading terms of its Taylor expansion,  $X(t)$  can be expressed as:

$$X(t) = X_{in} \left[ 1 + \frac{k_B T J_{c0}}{U_0 J_{c,in}} \ln \left( \frac{t}{\delta} \right) \right], \quad (2)$$

where  $X_{in} = wH/2H^*$ . (The additional factor  $J_{c0}/J_{c,in}$  has appeared as a result of eliminating the ill known  $t_0$  in favor of  $\delta$ .) Now consider what happens when the field is raised to  $H_2$  after having waited at  $H_1$  for the time  $t_w$ . The resulting flux-density profile is shown in Fig. 1(c).  $X'$  is the extrapolated penetration-depth of the steep portion (due to the second field change). The time evolution of  $X'(t')$  is also described by Eq. (2), where  $t'$  is measured from the time  $H_2$  is applied. The steep portion will meet the underlying old distribution when

$$X'(t') = X(t) = X(t' + t_w). \quad (3)$$

This is depicted in Fig. 1(d). Beyond this time all memory of the previous state is erased and the decay of the moment exhibits the usual logarithmic behavior for a direct field change from 0 to  $H_2$ . The crossover will occur at the time  $t'_i$  at which Eq. (3) is satisfied. Combining Eqs. (3) and (2) we arrive at the equation that relates  $t'_i$  to  $t_w$ ,  $T$ ,  $H_1$ , and  $H_2$ , which is the central result of this paper:

$$\left[ H_1 \ln \left( \frac{t'_i + t_w}{\delta} \right) - H_2 \ln \left( \frac{t'_i}{\delta} \right) \right] / (H_2 - H_1) = \alpha(T) = \frac{U_0 J_{c,in}}{k_B T J_{c0}} \quad (4)$$

Note that Eq. (4) for  $t'_i$  is valid as long as  $X$  is proportional to  $H$  and increases logarithmically with time—the result is independent of the specimen dimensions and geometry, as well as the shapes of the flux-density profile and flux front.  $M$  and  $dM/d(\ln t)$ , on the other hand, depend critically on all of these factors making their estimates less certain. Therefore in comparing measurements with theory, attention will be focused on  $t'_i$ .

The magnetization is given by  $4\pi M = -H + 2A/w$ , where  $A$  is the area under the profiles of Figs. 1. From the geometry of Fig. 1(c), and the expressions for  $X(t)$ ,  $X'(t)$ , and  $\alpha$  [Eqs. (2) and (4)], the time-dependent magnetization becomes

$$4\pi M = -H_2 + \frac{H_2^2}{2H^*} \left[ 1 + \frac{1}{\alpha} \ln \left( \frac{t'}{\delta} \right) \right] + \left[ \frac{1}{2H^* \alpha} \right] \left[ \alpha(H_1 - H_2) + H_1 \ln \left( \frac{t' + t_w}{\delta} \right) - H_2 \ln \left( \frac{t'}{\delta} \right) \right]^2 \left[ \ln \left( \frac{t' + t_w}{t'} \right) \right]^{-1} \quad (5)$$

The first term corresponds to the static Meissner term; the second term corresponds to the usual simple flux penetration and decay due to the application of a single field  $H_2$  upon the ZFC state; the third “memory” term is the contribution due to the underlying flux-density profile created by the first field change, and will tend to reduce the slope for times shorter than  $t'_i$ . For such times Eq. (5) predicts a very gradual departure from the  $t' \geq t'_i$  straight-line portion. To understand how the results are

affected when the profiles are not linear, we consider the rectangular shaped profiles shown in Figs. 1(e) and 1(f). An actual  $J_c(B)$  will decrease with field causing the flux-density profile to be steeper at locations deeper inside the sample, so that the shape will be intermediate between the two extremes of linear and rectangular profiles. As mentioned earlier  $t'_i$  is unaffected by differences in profile shapes, however, the behaviors of  $M$  and  $dM/d(\ln t')$  are changed significantly for  $t' < t'_i$ :

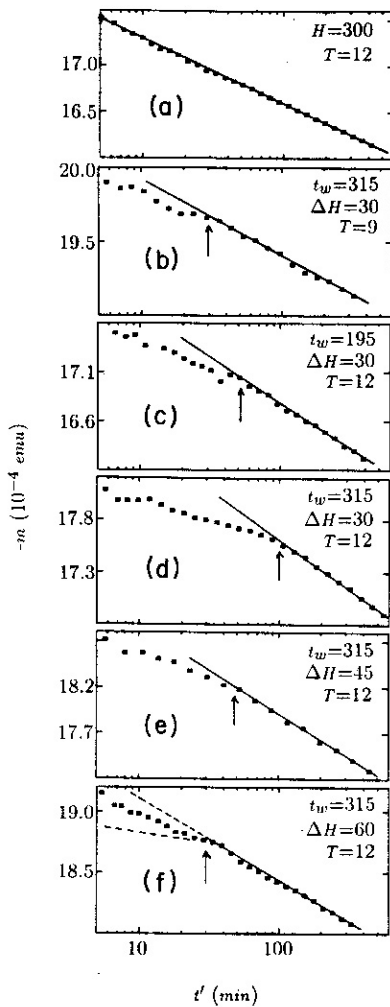


FIG. 2. Data for six runs.  $T$  is in K,  $\Delta H = H_2 - H_1$  in Oe, and  $t_w$  in min. The arrows show the positions of the crossovers ( $t' = t'_i$ ). For run (a) the field was directly stepped up from 0 to  $H_2$ . The broken lines in plot (f) correspond to predicted behavior for linear (upper) and rectangular (lower) profiles.

$$\begin{aligned}
 4\pi M = & -H_2 + \frac{H_2^2}{H^*} \left[ 1 + \frac{1}{\alpha} \ln \left[ \frac{t'}{\delta} \right] \right] \\
 & + \frac{H_1^2}{H^*} \left[ 1 + \frac{1}{\alpha} \ln \left[ \frac{t' + t_w}{\delta} \right] \right] \\
 & - \frac{H_1 H_2}{H^*} \left[ 1 + \frac{1}{\alpha} \ln \left[ \frac{t'}{\delta} \right] \right]. \quad (6)
 \end{aligned}$$

Equation (6) predicts a sharp inflection at  $t' = t'_i$ , an almost constant slope at shorter times and a more substantial change in slope than that predicted for linear profiles [Eq. (5)]—predictions which are self-evident from Figs. 1(e) and 1(f).

In the above calculations we have considered a single  $U_0$ . Extending the calculations of Hagen and Griessen,<sup>18</sup> we will assume that at a fixed temperature a finite distribution of  $U_0$ 's can be taken into account, by employing an effective  $\bar{U}_0$  given by

$$\left[ \int_{U_0^*}^{\infty} m(U_0) dU_0 \right] / \left[ \int_{U_0^*}^{\infty} m(U_0) / (bU_0) dU_0 \right],$$

TABLE I.  $\Delta H = H_2 - H_1$  is the increment in field;  $H_1 = 300$  Oe is the initial field for each run.  $t_w$  is the waiting time between applications of  $H_1$  and  $H_2$ . The  $t'_i$ 's are inflection times.  $\alpha_{\text{meas}}$  is the value of  $\alpha$  obtained from  $t'_i$ .  $\alpha_{\text{calc}}$  equals  $U_0 J_{c,\text{in}} / k_B T J_{c0}$ .

Run	$T$ (K)	$\Delta H$ (Oe)	$t_w$ (min)	$t'_i$ (min)	$\alpha_{\text{meas}}$	$\alpha_{\text{calc}}$
a	12					
b	9	30	315	27	24.9	28.2
c	12	30	195	55	13.8	13.3
d	12	30	315	98	12.6	13.3
e	12	45	315	47	12.5	13.3
f	12	60	315	30	13.3	13.3

where  $U_0^*$  and  $b$  are constants and  $m(U_0)$  is the distribution function.

The data are shown in Fig. 2 as plots of  $m$  versus  $\ln t'$ , the various runs having different sets of values of the parameters  $t_w$ ,  $T$ ,  $H_1$ , and  $H_2$ . These parameters and other relevant quantities for each run are shown in Table I. Plot (a) in Fig. 2 shows the usual smooth logarithmic decay when the field is stepped directly from 0 to  $H_2$  (300 Oe). The other curves show a change in behavior at some time  $t'_i$  (indicated by arrows), beyond which the curves become smooth and straight, and the slope steeper. Scatter in the data and rounding of the transition region make  $t'_i$  uncertain by  $\delta \ln t'_i \approx 0.4$ .

The  $t'_i$ 's show the trends expected from Eq. (4). Runs c and d have waiting times of 195 and 315 min respectively (same  $T$ ,  $H_1$ , and  $H_2$ ). As expected  $t'_i$  increases with  $t_w$ , although not in the simple manner predicted by the superconducting-glass model. Plots b (at 9 K) and d (at 12 K) show the expected variation with temperature for given  $t_w$ ,  $H_1$ , and  $H_2$ —the slower decay rate at the lower temperature gives rise to a smaller  $X(t_w)$  and hence  $X'$  has a smaller distance to cover before it overtakes  $X$ . Plots d, e, and f correspond to field increments of 30, 45, and 60 Oe, respectively ( $H_1 = 300$  Oe,  $T = 12$  K, and  $t_w = 315$  min in each case). As can be seen,  $t'_i$  decreases as  $\Delta H$  is increased because  $X'$  increases with  $\Delta H$ , bringing it closer to  $X(t_w)$ .

To make a quantitative comparison with the model, the parameter  $\alpha(T)$  of Eq. (4) is obtained in two ways:  $\alpha_{\text{calc}}$  (shown in column 7 of Table I) is calculated from the right-hand side and known values of  $J_{c,\text{in}}$ ,  $J_{c0}$ , and  $U_0$ ;  $\alpha_{\text{meas}}$  (column 6) is from the observed  $t'_i$  and the left-hand side of Eq. (4). In earlier work<sup>7</sup> we found  $U_0 = 0.046$  eV and

$$J_{c,\text{in}} = (4.74 - 0.278T) \times 10^4 \text{ A/cm}^2$$

( $J_{c,\text{in}}$  was called  $J_{c,x}$  there).  $\delta$  has been chosen to be 15 min (for consistency with the earlier work), but the results are not sensitive to its choice. As can be seen from the table, the "measured" ( $\alpha_{\text{meas}}$ ) and "calculated" ( $\alpha_{\text{calc}}$ ) values are in reasonable agreement. It was found that the data were not reproducible for much shorter or much longer times. The error involved in defining the zero of time is probably responsible for the former, whereas limi-

tations to the long-term stability of the decay rate (possibly caused by temperature and mechanical disturbances) may restrict the maximum reproducible experimental time. Similarly the field increment had to be at least 30 Oe for reproducible results. Because of the limitations on time and  $\Delta H$ , it was not possible to obtain reliable data at much lower temperatures (the slower decay rates demand unacceptably long waiting times). At higher temperatures (e.g., 50 K) the magnetization becomes predominantly reversible (the irreversible component vanishing above the irreversibility line<sup>7</sup>), and the signal-to-noise ratio very small ( $H^* \sim 100$  Oe). As a result of the latter we could not determine whether the relaxation was exhibiting any memory effect.

In the regime  $t' < t'_i$ , the behavior of the data is intermediate to that predicted for the linear [Eq. (5)] and rectangular [Eq. (6)] profiles and therefore corresponds to a physically reasonable  $J_c(B)$ . As an example, this is illustrated on plot  $f$  in Fig. 2, where the broken lines correspond to Eqs. (5) and (6). Obtaining more information about  $J_c(B)$  from the data in the  $t' < t'_i$  region is difficult

because of the scatter and inherent inaccuracy of that data, and the additional assumptions that must be made regarding sample and flux-front geometries.

In conclusion we have shown that, with flux creep in a superconductor, the application of two consecutive field changes separated by a long waiting time will, under certain conditions, create a two-component decaying flux distribution. The decay of this compound state will show a crossover in behavior at a time  $t'_i$ , when the memory of the first flux distribution is erased. Because the derivation depends in such an essential way on the picture [portrayed in Figs. 1(a) and 1(b)] of well-defined flux-density profiles, and flux fronts that gradually propagate into the sample, the qualitative trends exhibited by the data support that picture. Although, because of its more complicated nature, it is not inconceivable that a sophisticated treatment of the superconducting-glass model (which is beyond the scope of the present work) might be able to explain our observations, the quantitative agreement that we see indicates the validity of the conventional flux-creep model, at least at low temperatures.

- <sup>1</sup>K. A. Müller, M. Takashige, and J. G. Bednorz, *Phys. Rev. Lett.* **58**, 1143 (1987).
- <sup>2</sup>C. Ebner and D. Stroud, *Phys. Rev. B* **31**, 165 (1985).
- <sup>3</sup>Y. Yeshurun and A. P. Malozemoff, *Phys. Rev. Lett.* **60**, 2202 (1988).
- <sup>4</sup>C. P. Bean, *Phys. Rev. Lett.* **8**, 250 (1962).
- <sup>5</sup>Y. B. Kim, C. F. Hempstead, and A. R. Strnad, *Phys. Rev. Lett.* **9**, 306 (1962); *Phys. Rev.* **129**, 528 (1963); W. A. Fietz, M. R. Beasley, J. Silcox, and W. W. Webb, *ibid.* **136**, A335 (1964).
- <sup>6</sup>A. P. Malozemoff, L. Krusin-Eibaum, D. C. Cronmeyer, Y. Yeshurun, and F. Holtzberg, *Phys. Rev. B* **38**, 6490 (1988).
- <sup>7</sup>B. D. Biggs, M. N. Kunchur, J. J. Lin, S. J. Poon, T. R. Askew, R. B. Flippen, M. A. Subramanian, J. Gopalakrishnan, and A. W. Sleight, *Phys. Rev. B* **39**, 7309 (1989).
- <sup>8</sup>P. W. Anderson, *Phys. Rev. Lett.* **9**, 309 (1963); P. W. Anderson and Y. B. Kim, *Rev. Mod. Phys.* **36**, 39 (1964); M. R. Beasley, R. Labusch, and W. W. Webb, *Phys. Rev.* **181**, 683 (1969).
- <sup>9</sup>A. M. Campbell and J. E. Evetts, *Adv. Phys.* **21**, 199 (1972).
- <sup>10</sup>M. E. McHenry, M. P. Maley, E. L. Venturini, and D. L. Ginnley, *Phys. Rev. B* **39**, 4784 (1989); M. E. McHenry, M. P. Maley, G. H. Kwei, and J. D. Thompson, *ibid.* **39**, 7339 (1989).
- <sup>11</sup>David R. Nelson, *Phys. Rev. Lett.* **60**, 1973 (1988); Matthew P. A. Fisher, *ibid.* **62**, 1415 (1989); V. G. Kogan and L. J. Campbell, *ibid.* **62**, 1552 (1989).
- <sup>12</sup>P. L. Gammel, L. F. Schneemeyer, J. V. Waszczak, and D. J. Bishop, *Phys. Rev. Lett.* **61**, 1666 (1988); S. Gregory, C. T. Rogers, T. Venkatesan, X. D. Wu, A. Inam, and B. Dutta, *ibid.* **62**, 1548 (1989); G. J. Dolan, F. Holtzberg, C. Feild, and T. R. Dinger, *ibid.* **62**, 2184 (1989).
- <sup>13</sup>C. Rossel, Y. Maeno, and I. Morgenstern, *Phys. Rev. Lett.* **62**, 681 (1989).
- <sup>14</sup>M. A. Subramanian, C. C. Torardi, J. C. Calabrese, J. Copalakrishnan, K. J. Morrissey, T. R. Askew, R. B. Flippen, U. Chowdhry, and A. W. Sleight, *Science* **239**, 1015 (1988).
- <sup>15</sup>J. J. Lin, E. L. Benitez, S. J. Poon, M. A. Subramanian, J. Gopalakrishnan, and A. W. Sleight, *Phys. Rev. B* **38**, 5095 (1988).
- <sup>16</sup>P. Chaddah and G. Ravikumar (unpublished).
- <sup>17</sup>P. Kes, J. Aarts, J. van den Berg, C. J. van der Beek, and J. A. Mydosh, *Supercond. Sci. Technol.* **1**, 242 (1989).
- <sup>18</sup>C. W. Hagen and R. Griessen, *Phys. Rev. Lett.* **62**, 2657 (1989).